Micro-movements and micro-pump-effect of Implant-abutment-connection

Test-Report

for Konus K3Pro Dental Implants

Department of Prosthetic Dentistry

J. W. Goethe-University Frankfurt am Main

Director: Prof. Dr. H.-Ch. Lauer

Dipl.-Ing. H. Zipprich

Address:

Theodor-Stern-Kai 7,Haus 29

60596 Frankfurt a. Main

Datum: **15. Juli 2010** Fax.: (069) 6301-3711

E-Mail: Zipprich@em.uni-frankfurt.de Tel.: (069) 6301-4714

Directory

1 Material and method

In order to examine the existence of a micro pump on dental implants; a special experimental test field was developed. For each type of implant-system tested; five inspection pieces were manufactured. Each inspection piece simulates an implant-supported molar crown in the upper jaw. The surrounding mucous membrane at the Implant-Abutment-Interface was duplicated by a Polyether impression material. A liquid entrance was created inside each of the artificial mucous membranes and a specifically developed x-ray contrast medium was used and brought into the opening. During the load, in a two-dimensional chewing simulator, a constant and diverging X-ray device radiated the inspection pieces. By transformation of the x-ray into visible light; x-ray videos were recorded, using a high speed digital camera. The results will give information on the development and a conclusion of a micro pump effect at the implant Abutment interface.

2 Experimental setup

Illustration 1 shows schematically the experimental setup. Those in the x-ray source: [1] analysation of an exemplary inspection piece loaded in a two-dimensional chewing simulator [3] [2; 4]. The x-rays are converted in the image amplifier [5] into visible light. The quantity of light coming from the image amplifier meets the CCD sensor of the High speed digital camera [6]. Afterwards; the camera sends a digital signal to an attached computer, whereas the computer then developes x-ray-videos on the processes of the Implant-Abutment-Interface.

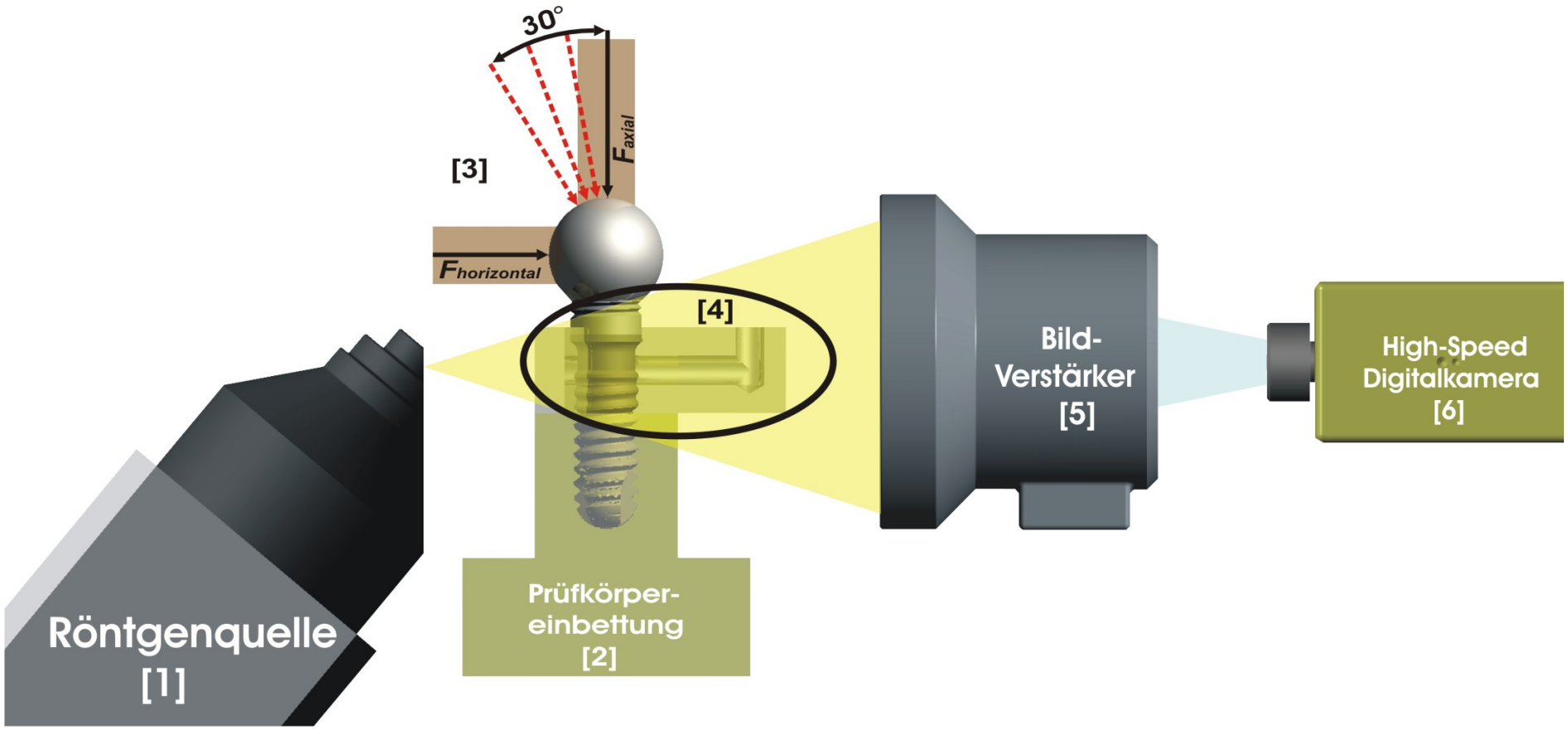

Fig. 1:
Schematic representation of the experimental setup. [1] = source of x-ray [2] = embedded inspection piece [3] = chewing simulator [4] = saliva replacement/ x-ray contrast medium [5] = radiograph amplifier [6] = High speed digital camera

2.1 Source of x-ray

In the, here described, investigation an x-ray unit type FXS-160.50 was used. (Fine focus of X-Ray systems, www.yxlon.de). Fig. 2 shows a schematic diagram of the x-ray unit used.

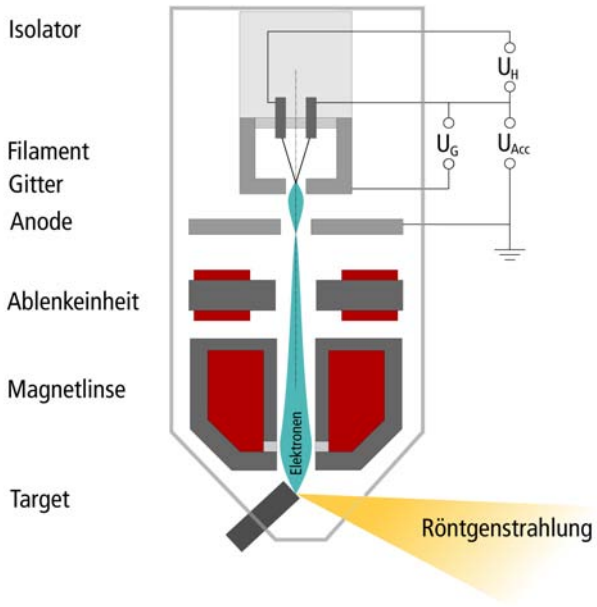

Fig. 2:
Schematic structure of the x-ray tube.

Used specific data for the source of x-ray are the Tab. to infer 1a and b.

Radiation characteristic	▪ Emission angle: 40° ▪ rotational target Target material: Tungsten with beryllium filter

Tab. 1a: Specific data of the x-ray source.

Ranges	▪ Tension 5 - 160 kV ▪ Target stream 0 - 1,0 mA ▪ Continuous duty (+ Cooling): 160 Watt ▪ Focal spot size adjustable 3 - 1000 µm

Tab. 1b: Specific data of the x-ray source.

The applied x-ray unit is a constant emitter, with which the x-radiation spreads divertingly. Divertional spreading of the radiation, leads to an enlargement of the radiated object (see fig. 3).

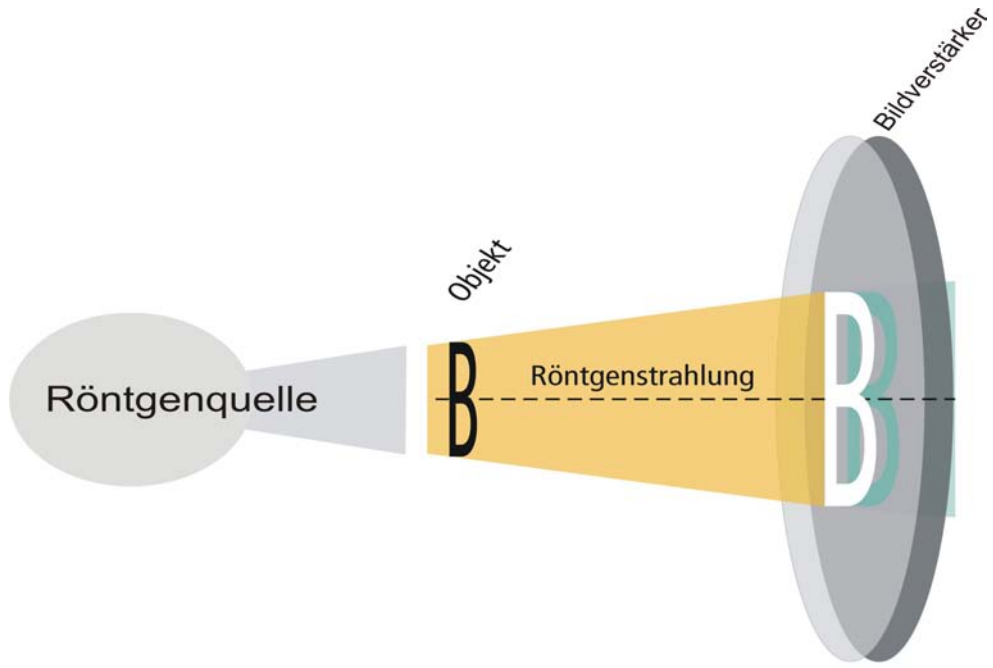

Fig. 3: Geometrical conditions the object radiograph amplifiers of source of x-ray.

The focal spot size can be adjusted up to 3 µm (Tab. 1) and therefore leads to a theoretical resolution of maximum 3 µm. To note though is however; that the bulb *power* needs to reach 16 Watts, to allow for a manuall adjustment of the focal spot of 3 µm. The increase and achievement of over 16 Watts automatically leads to an enlargement of the focal spot and concomitantly reduction of the resolution. In the investigation; a maximum output of 16 Watts was used. A lead screen was used to avoid stray radiation. In the

available test series; an underlying closed voltage of 120 keV and a current of 0,1 mA was used. The output is calculated with and results in 12 Watts.

2.2 Inspection piece

Tab. 2 showes the tested implant-components.

compnents	**measurement**	**reference no.:**	**LOT no.:**
implant	Konus K3Pro 4,5mm x 13mm	45013K3 Pro/ET	602224-24
abutment incl. binding-screw	Konus K3Pro 5,0 x 1,5mm 0°	EA 500015.H/3Pro	7397

Tab. 2: tested implant-components.

In fig. 4 an inspection piece is exemplarily represented. Thereby the implant body is embedded in a resin block (Technovit® 4004). The impression-material of Polyether (Impregum™) surrounds the implant Abutment connection as a simulation for the periimplant tissue. The force application is loaded through an aluminium fabricated ball top, which is screwed and glued to the implant/ abutment sample.

Fig. 4:
Inspection piece.

Fig. 5 shows an exemplary sample inspection piece in the diagonal view. The simulated gingiva is composed of impression-material Impregum™, within which a liquid channel was created. This entrance channel reaches up to the implant/ abutment connection and serves as reservoir for a saliva-similar liquid.

Fig. 5: Inspection piece in diagonal view.

In fig. 6 the inspection piece is shown from the top-view. Perpendicularly; the liquid channel for the relief of pressure becomes visible.

Fig. 6:
Inspection piece from above.

2.3 Production of the inspection pieces

The production of the inspection pieces required some preparing measures, which are explained in the following:

Production of cementation caps

The cemented caps consist of aluminium, which were applied on each abutment by means of attachment; using autopolymerizing composits (3M Espe Nimetic™ Cem; www.espe.de). The manufacturing of all cemented caps took place through a centrifical lathe (company emco Austria, emcotronic TM02 and emco turn 120). The aluminium caps have an inside diameter of 3,5mm, are 6mm in length and have an internal thread (M5 x 0,5mm) of variable length. Fig. 7 shows exemplarily two cementing caps. The caps serve as assistance for the screwing of the load attachments, which are described in the following.

Fig. 7: Cementing caps from aluminum.

Preparation of the Abutments

The original abutments were manufactured under manufacturing specifications and diameters (see Tab. 2). For the available investigation all abutments were milled to a diameter of 3,45mm in a centre lathe (company emco Austria, emcotronic TM02 and emco turn 120). Subsequently, all abutments were sandblasted carefully with commercial blasting equipment. This measure served as reinforcement for the glued connection between the cementing cap and the Abutment. Fig. 8a shows an exemplary abutment before milling, whereas fig. 8b shows the same Abutment after lathing and sand blasting.

Fig. 8a: Implant with a non-milled original Abutment.

Fig. 8b: Lathed Abutment including the fixation screw.

Assembly of the Abutments

The milled and blasted Abutments were fixed to the implant using the manufacturer's specifications (Argon-Medical 25Ncm). A calibrated torque wrench Torsiometer 760 (www.stahlwille.de) was thereby used. Fig. 9 shows the torque wrench used and all recommended manufacturing tightening torques were followed.

Fig. 9: calibrated torque wrench.

Production of the load attachment

The load attachment for the enossale implant abutment was designed spherically. A loading ball cap attachment was manufactured for each inspection piece. The ball attachment consists of aluminum and has an outside diameter of 8,0mm. In fig. 10 a load attachment (loading ball cap) is represented.

Fig. 10: load attachment.

The internal thread of the load ball fits the external thread of the cementing cap. This allows for a variable length of the ball height and an adjustment of the lever arm length. Fig. 11 shows the load attachment screwed onto the cementing cap. In order to ensure a

firm seat of the spherical load attachment, a PTFE sealant strip was applied on the external thread of the cementing cap.

Fig. 11: Cementing cap with a screwed on load attachment.

Production of the embedding mold

In order to standardise the embedding of the implants; an embedding mold was manufactured for all units tested. The production of the mold always followed same protocol. A T-fitting block of aluminum (T1) was manufactured for each implant system. The block (T2) served as negative for the manufacturing of the T-fitting units using Technovit® 4004, in which each implant tested was embedded. In T1 a preparatory implant was set. The positioning and measurements used are shown in Fig. 12.

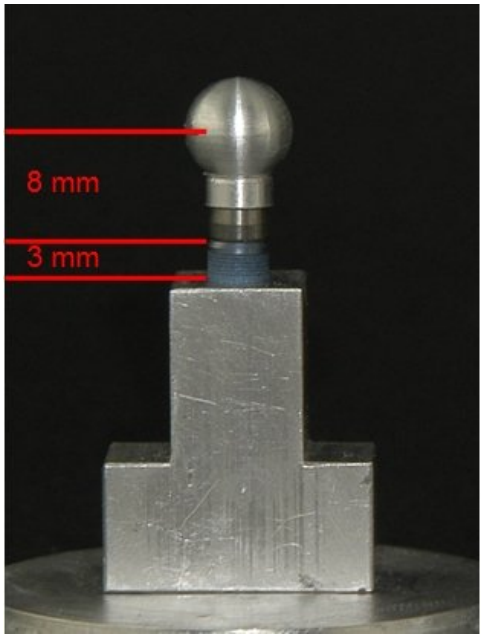

Fig. 12: In the T-fitting (T1) positioned implant.

The embedding form was manufactured using silicon (Copie sil® 18 basis and catalyst, dentona AG Dortmund). In addition; a cylindrical-form using aluminum was designed and manufactured as a container for molding. The designated implant was attached at the base of the cylindric-form T1, (Fig. 13), using a screw fixation.

Fig. 13: Embedding form with T1 and implant.

After attachment and screw fixation, the cylindrical-form was then filled from above using silicon (Copie sil® 18 basis and catalyst, dentona AG Dortmund) in (fig. 14).

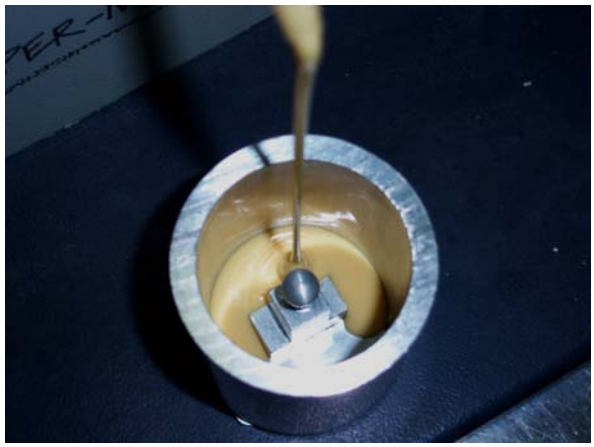

Fig. 14: puring of the silicon into the mold.

After disassembly of the cylindrical-form and removal of the base, by loosening of the retention screws from T1, the T-fitting unit could be easily removed from the

manufactured embedding mold, due to the high elasticity of the silicon. Such a mold served as embedding device for each individual implant, so that an embedding mold was manufactured for the implant system. In Fig.15a and b the sectional view of an embedding mold is shown.

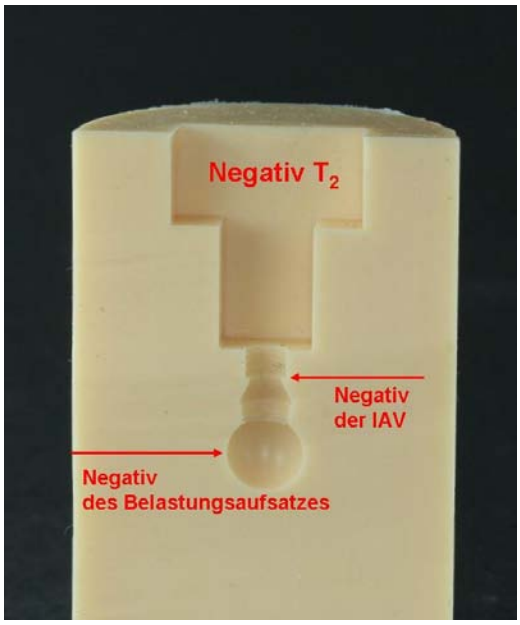

Fig. 15 a: Sectional view of an embedding mold.

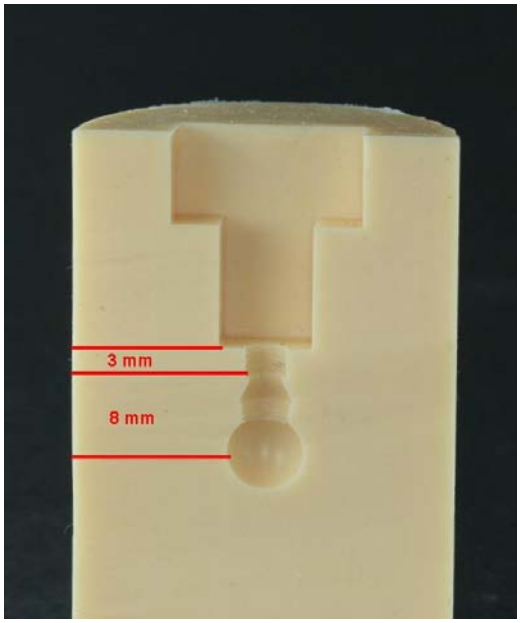

Fig. 15 b: Distances within the embedding mold. Representation for the norm DIN 14801.

Each implant in the study was prepared using the descriptive approach for the embedding of the implant bodies.

The implant body embedding

The result of the preparation measures is a system-specific embedding process, for an enossal implant with a definitely attached abutment. On this prosthetic post the cementing cap is fastened and the load attachment is screw-fixed in such a way that the measurements requirements are fulfilled; as shown in fig. 15 b. In fig. 16 finally prepared implant is to be shown by the example of an Konus K3Pro implant.

Fig. 16: Implant with cemented cap and load attachment (ball).

With the help of the manufactured molds the implants could be embedded, using the transparent, 2-component material on basis of Methylmethacrylat, in form of powder and liquid (Technovit® 4004; www. kulzer technik.de). The screwed ball cap (load attachment) ensures an accurate positioning of the implant in the embedding mold (fig.17a and b).

Fig. 17a: Implant positions in the embedding mold; Sectional view. Fig.

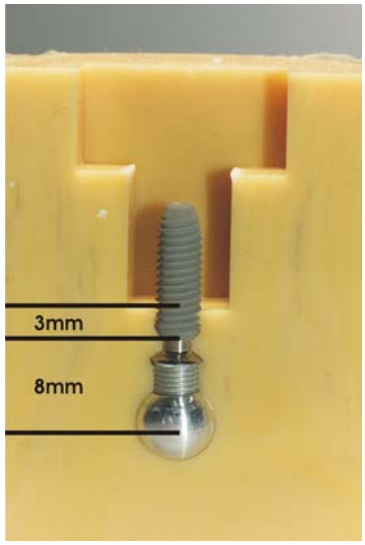

Fig. 17b: Realization of the norm DIN 14801.

After positioning of the implant in the embedding mold, the cavity (T-fitting) was filled with resin (Technovit® 4004; www.kulzer-technik.de). Fig. 18 shows an implant in the embedding mold and Fig. 19 shows the filling of the cavity with resin.

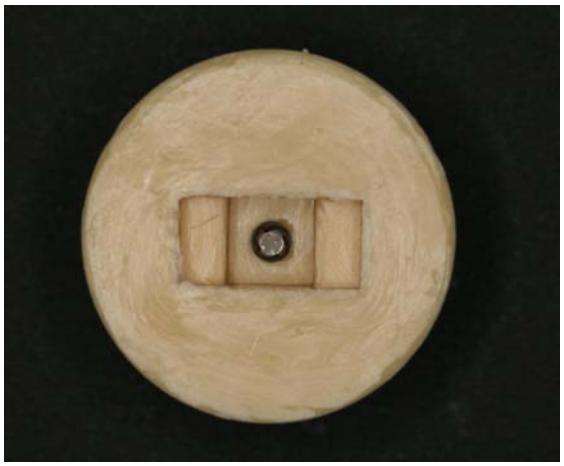

Fig. 18: Implant in the embedding mold; View on the apical portion of the implant.

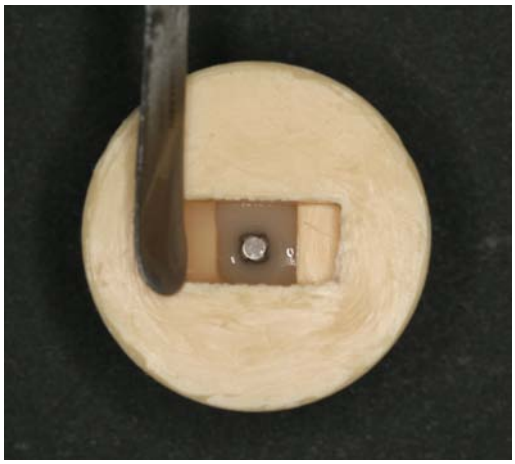

Fig. 19: Filling of the embedding mold with resin.

After the polymerization (manufacturer data 4-6 min.) the implant was firmly embedded in the resin and could be removed from the form. Fig. 20 represents an implant after removal from the mold. The load distance, defined by the distance from the ball center up to the implant shoulder, is a consistant 8mm (tolerance +/− 0,1mm). The height of the embedded implant body corresponds to the portion of the implant, which is clinically embodied in the bone. Following the DIN EN ISO 14801 a boneloss was of 3mm was simulated.

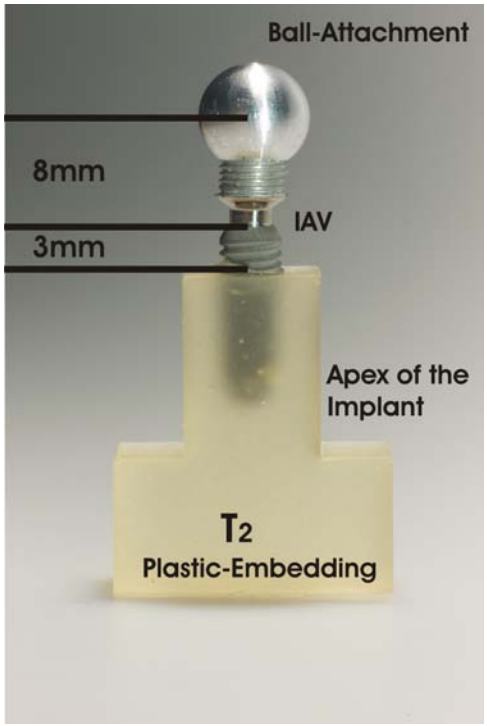

Fig. 20: Directly after releasment from mold. Embedded implant with load attachment (ball cap). DIN 14801 illustration.

This embedding-material was selected because its' module of elasticity (elastic module) of approximately 2000 - 2300 N/mm2 (Technovit® 4004, www.kulzer-technik.de) and is therefore a little over the value of Human Spongiosa. Human bone values are known to be between 1000 N/mm2 (Spongiosa) and 10000 N/mm2 (Cortical). In the herein examined study an implant-supported molecular crown of the upper jaw was simulated. The maxilla consists in large of Spongiosa; whereas the Corticalis, with its' compact structure, constitutes only a small portion. Therefore the Corticalis under clinical conditions surrounds a smaller part of the implant body than the Spongiosa. Elastic module of the herein used embedding-material was selected so that it resembles the elastic module of the Spongiosa. The influence factor of the Corticalis was thereby considered.

Simulation of the gingiva

A surrounding membrane; that simulates the mucous around the enossales implant is to be duplicated in this study. The following parameters were crucial with the choice of the material:

- Good shelf-life
- Sealing of the IAI, but no sticking at the surface of the implant
- No interaction with the X-ray contrast medium and/or saliva substitute
- Easy processing
- Fast setting

In first preliminary tests the irreversible hydraulic colloid Alginat® was used. The easy handling and fast setting was favourable, however the bad shelf-life led to a high number of inspection pieces that had to the excluded. Beyond that; it showed that the x-ray contrast medium, or the saliva substitute, was partly resorbed by the Alginat®. In the next stage different Silicon's, used in the dentistry, was tested. The handling was acceptable in all cases; however, in all cases, the sealing was insufficient around the IAI. A silicon caoutchouc (rubber) used in hobbycraft (hobby time silicon caoutchouc rubber RTV/HV, Glorex OF Switzerland) exhibited good sealing properties; however the complicated handling was not applicable in a large number of the inspection pieces. With the material of Polyether Impregum™ (3M Espe, www.espe.de) all demanded parameters could be

obtained. In dentistry Impregum™ is used for casting of inlays, onlays, crowns, bridges, and veneers; as well as for functional registration, fixation, and use in implant casting. The selected material was placed in and around the preparatory implant. In order to test the IAI, it was necessary to manufacture a direct entrance to the Implant-Abutment-Interface (IAI). Fig. 21 points the schematic arrangement of the artificial mucous membrane, the IAI and the entrance channel to the IAI.

Fig. 21: Schematic arrangement of the IAC, the artificial mucous membrane and the entrance channel to the IAC.

In order to ensure a direct entrance to the IAI, a prefabricated sealing rod, made of brass, was individualized for each IAI. Using the sealant rod and within the inside of the imitated mucous membrane; a liquid entrance could be formed to the IAI. The sealing rod exhibited an outside diameter of 2mm. In order to optimize the sealing properties, an individualisation took place, with dental gutta-percha. An impression of each IAI could therefore be provided (fig. 22).

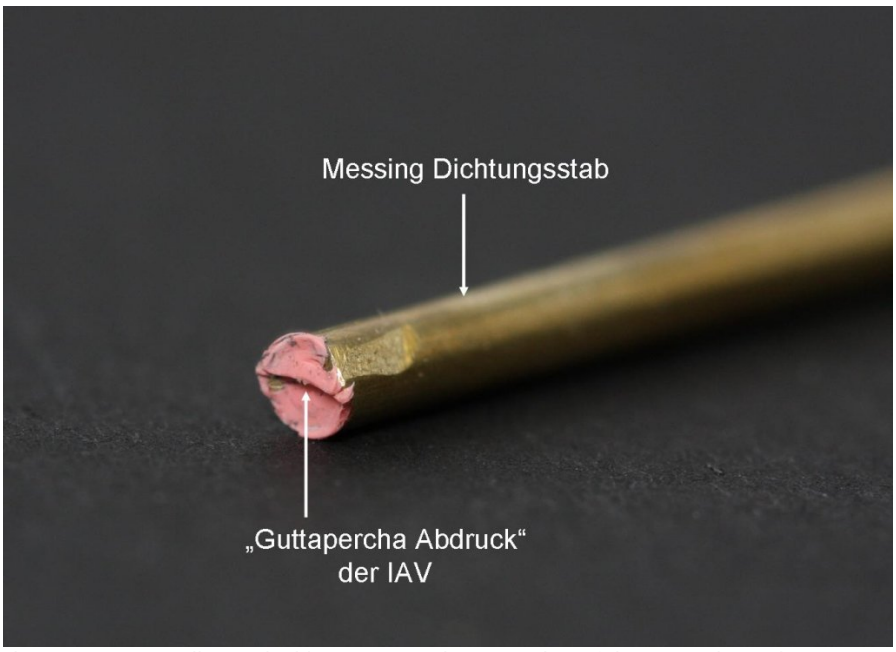

Fig. 22: Brass sealing rod with „gutta-percha “- casting of the IAC. The rod serves as a sealant of the IAC and liquid entrance to the IAC.

For the positioning of the artificial mucous membrane an embedding device, made of aluminium, was designed and manufactured (fig. 23).

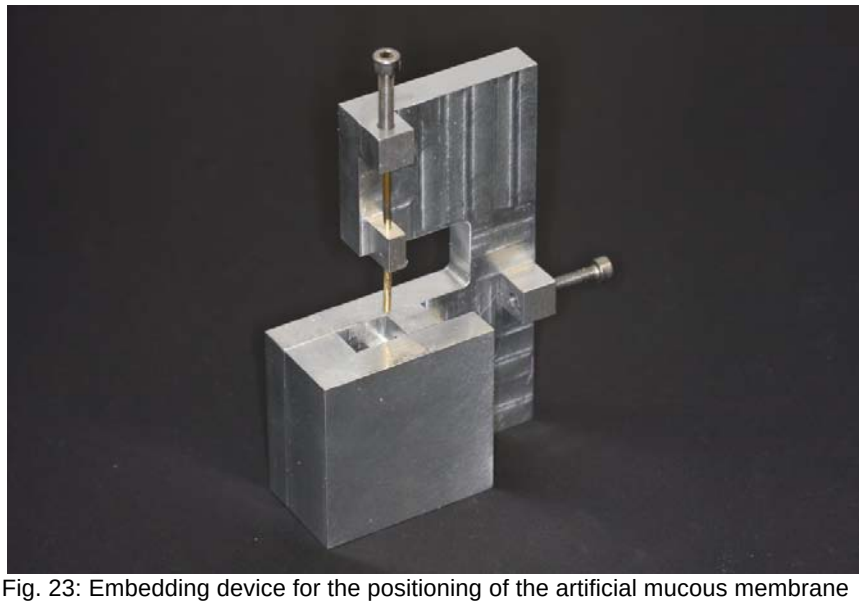

Fig. 23: Embedding device for the positioning of the artificial mucous membrane around the IAC.

The construction of the embedding device notes the exact positioning of the embedded implant (fig. 24).

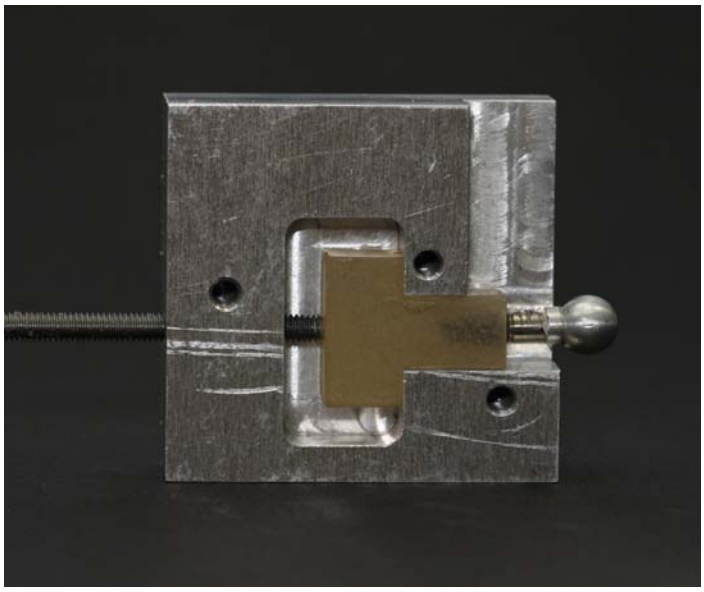

Fig. 24: Placement of the implant (embedded in resin) in the embedding device.

A, exactly planned, drilled entrance allows for an accurate clamping of the sealing rod. An added rod is attached perpendicular to the sealing rod, for the purpose of a pressure balance. Fig. 25 a. and b shows a detailed view of the rod arrangement in the embedding device.

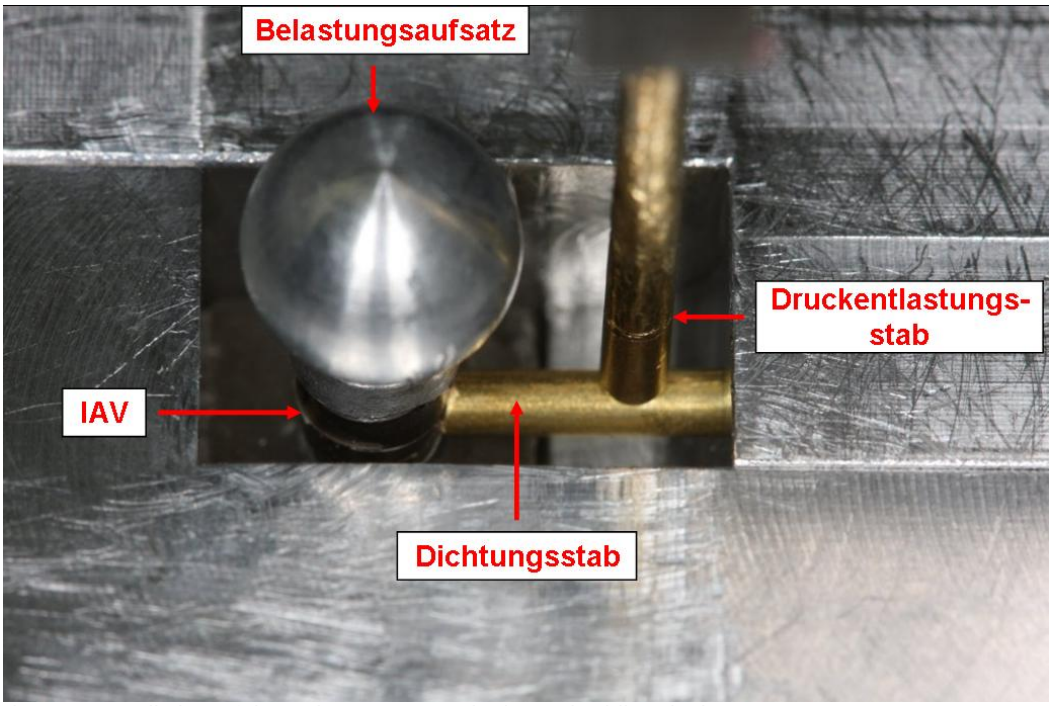

Fig. 25a: Detail view of the rod arrangement in the embedding device.

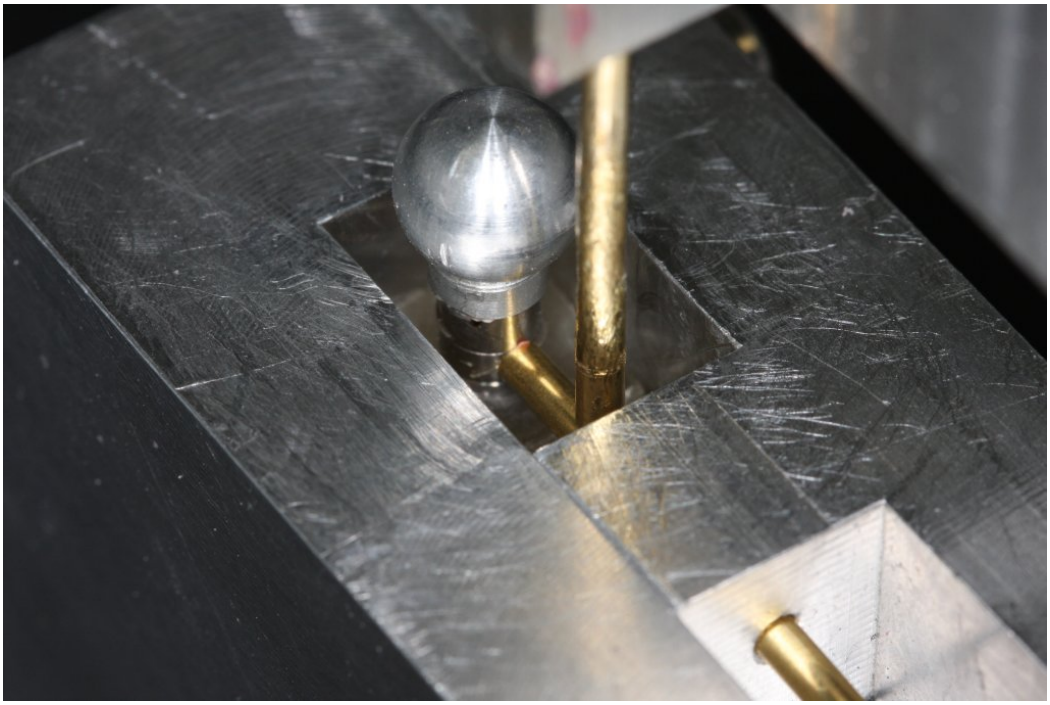

Fig. 25b: Detail view of the rod arrangement in the diagonal view.

The placement of the Impregum™ takes place with a prefabricated applicator (fig. 26a and b).

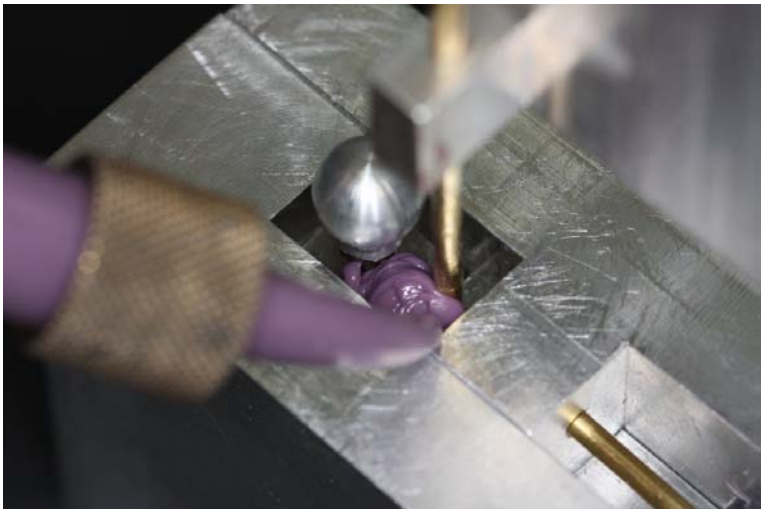

Fig. 26a: Placement of the Impregums™ to the mucous membrane imitation.

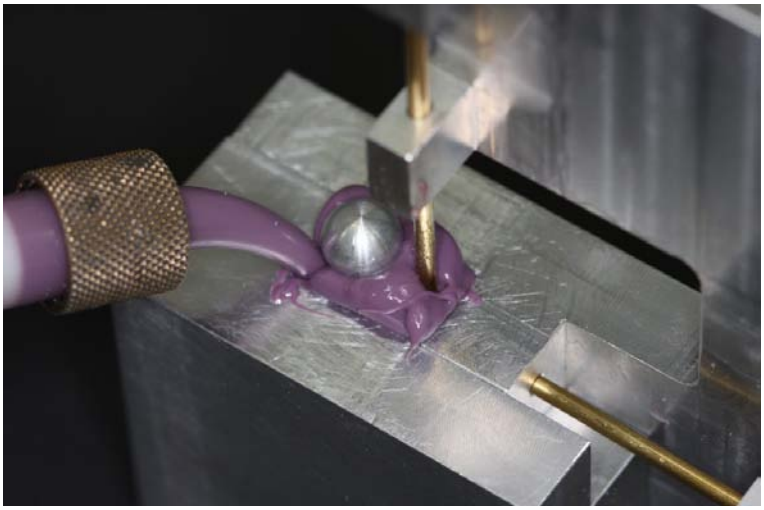

Fig. 26b: Filling of the embedding device with Impregum™ to the mucous Membran-imitation.

Fig. 26 b: Filling of the embedding device with Impregum™ to the mucous Membran-imitation.

After the prescribed setting time of seven minutes, the sealing rod was removed. Removal of the sealing rod leaves an entrance channel for the, later to be brought-in, x-ray contrast liquid. Fig. 27 shows the artificial mucous membrane in the profile. For this representation the implant was removed.

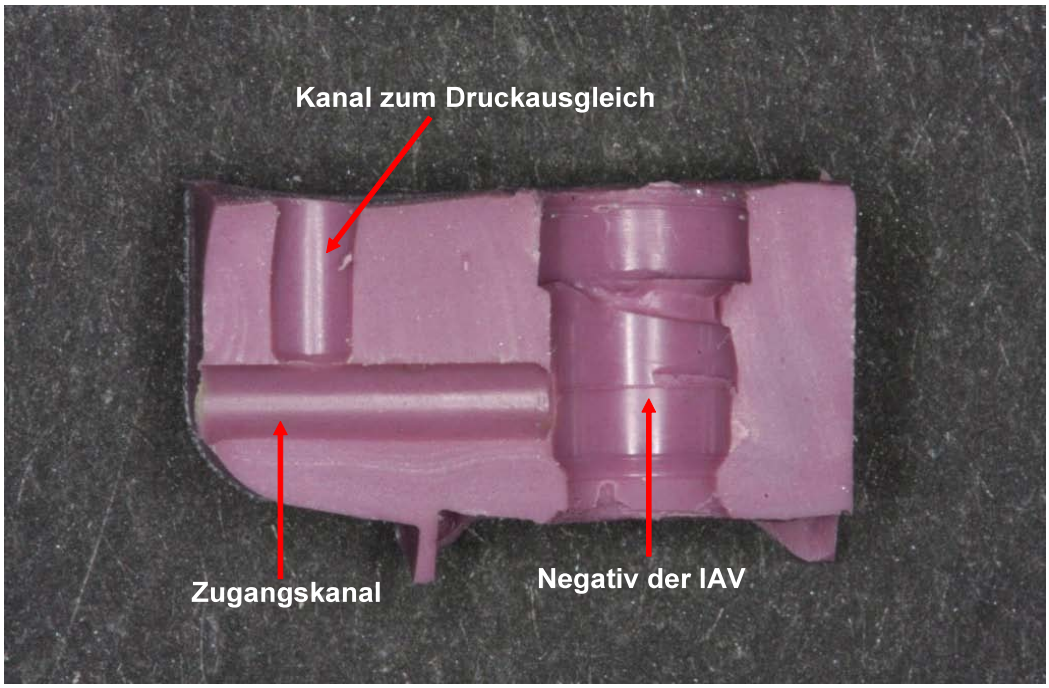

Fig. 27: Profile by the artificial mucous membrane.

The implant and the sealing rod were previously removed. In the center of the entrance channel lays the implant Abutment connection. In fig. 28 the inside view of the entrance channel is shown.

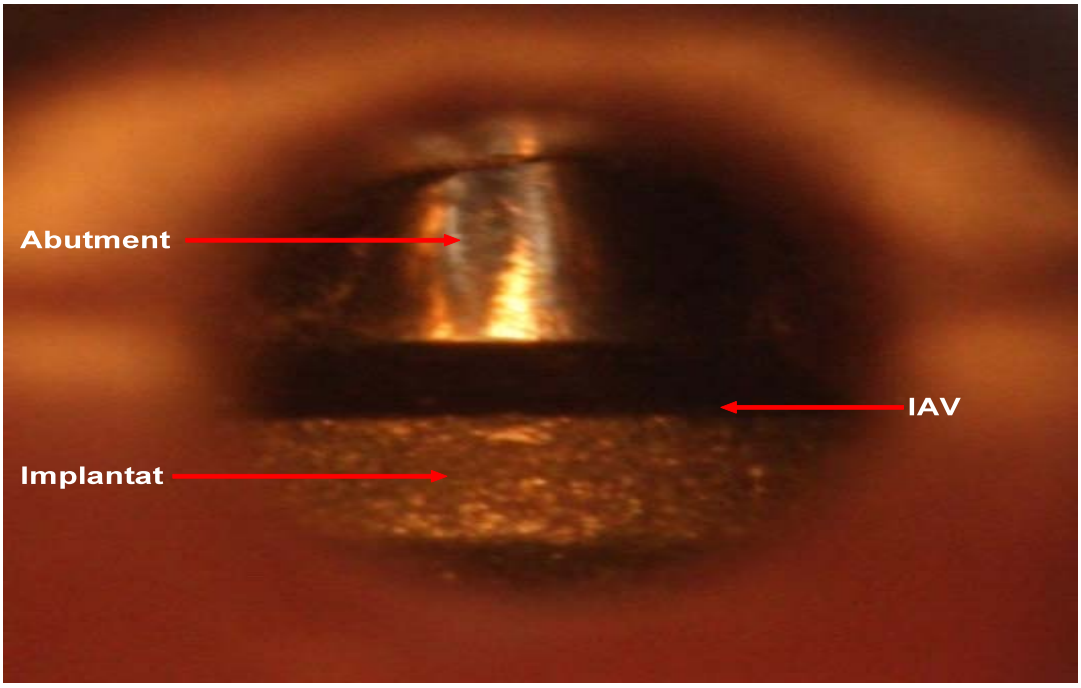

Fig. 28: View into the entrance channel to the IAC.

2.4 Saliva replacement / x-ray contrast liquid

The imitation of human saliva is possible by the use of saliva substitutes. Different basis materials exist. Due to the saliva-similar wetting characteristics; in the prescribed study a saliva substitute was used on the basis of mucin. The inspection piece was radiated during the force application with x-ray. The used saliva substitute is not visible with an x-ray device; so that in order to be able to observe the dynamic behavior of this liquid, the saliva substitute had to be made visible under x-ray examination. At the same time the wetting characteristics of the liquid should be similar to that of the human saliva.

2.4.1 Theoretical bases to the wettability

The wettability describes the behavior of a liquid in contact with the surface of a solid body. An applied liquid drop on a horizontal, even surface illustrates the wetting on this solid body. The wetting characteristic is described over the contact angle. The contact angle is firmly/liquid/gaseous the angle between the base line of a liquid drop and the tangent at the 3-phase point (fig. 29).

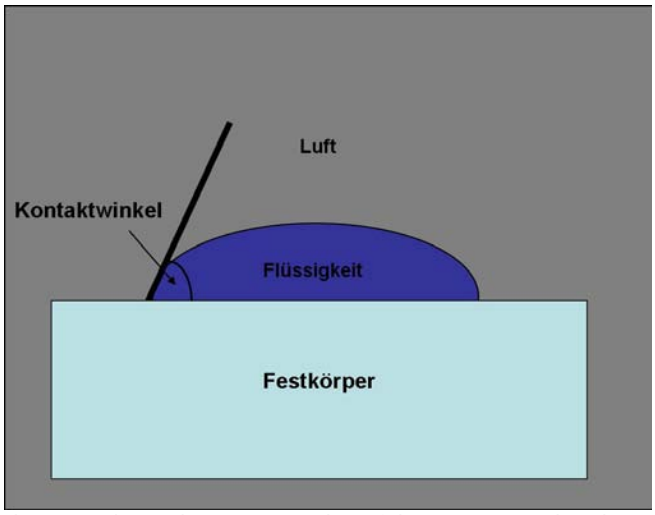

Fig. 29: Schematic representation of the contact angle. The contact angle informs about the wettability.

The contact angle can have values within the borders between 0° - 180°. A liquid works moistening, if the contact angle amounts to < 90°. Contact angle > 90° means non-wetting. The values 0° or 180°, total or non-wetting, do not arise in the reality.

2.4.2 Determination of the contact angle

At present there is no known scientific data over the contact angle between human saliva and a titanium surface. In order to have a reference or value for the contact angle for the liquid used here; the contact angle for saliva on a titanium surface was determined.

Therefore four human saliva samples were taken. Each sample was taken in the period of: after lunch, but before dinner. All samples taken, provided a total of 5 ml of human saliva. The second sample amount, of likewise 5 ml, consisted the use of a saliva substitute (Saliva medac® www. medac.de). The third sample contained the non-ionic x-ray contrast meadium Iomeporol (Imeron 300® injection solution www.bracco.de). The saliva substitute containing iodine Imeron 300® is used in medicine for CT-supported contrast central photographs of the head and for the representation of body cavities. The concentration of the x-ray contrast medium was prepared in such a way that an x-ray-difference between the liquid and its environment; here the artificial mucous membrane and the implant, was realized. Three contact angle measurements were conducted for each sample and afterwards the arithmetic mean value was calculated. The measurement was carried through with the Krüss Drop Shape Analysis System DSA10 MK2 (www.krüss.de). With a hollow needle (outside diameters 0,5mm) a liquid drop of the respective sample was dropped on a titanium surface and the contact angle was determined. The measuring temperature amounted to 21°. The contact angulation measurement was conducted by the company Pfeiffer (www.pfeiffer.de). In the illustrations 30 a, b and c are representations of the placement of liquid drops on the titanium surface.

Fig. 30a Sample 1 human saliva.

Fig. 30b Sample 2 artificial saliva.

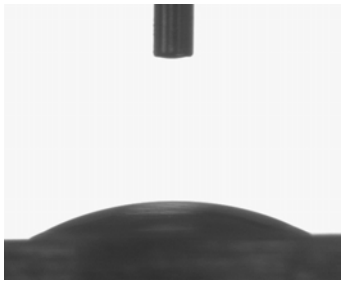

Fig. 30c Sample 3 artificial. Saliva + X-ray contrast medium.

The result of the contact angular measurement is represented in Tab. 3.

Sample 1 (human saliva)	**Sample 2** (artificial saliva)	**Sample 3** (artificial saliva **+** X-ray contrast medium.)
48,3°	58,1°	46,7°
51,3°	57,8°	48,3°
53,3°	63,6°	46,8°
average = 50,96°	**average = 59,83°**	**average = 47,26°**

Tab. 3: Results of the contact angular measurement.

The results of the contact angular measurement show that the wetting characteristic of the used liquid (artificial saliva + Roentgen contrast medium) is similar to the wetting characteristics of the reference liquid (human saliva).

2.5 Chewing simulator

In the available investigation a two-dimensional chewing simulator was used. „The Frankfurt chewing simulator “was designed and built particularly for testing of Implant Abutment connections (IAI). It makes the application of two-dimensional chewing forces possible. On the inspection samples and/or on the IAI, the influencing force is produced by two electro-dynamic force actuators. These are arranged in right-angles to one another in the „Frankfurt chewing simulator “ (Fig. 31).

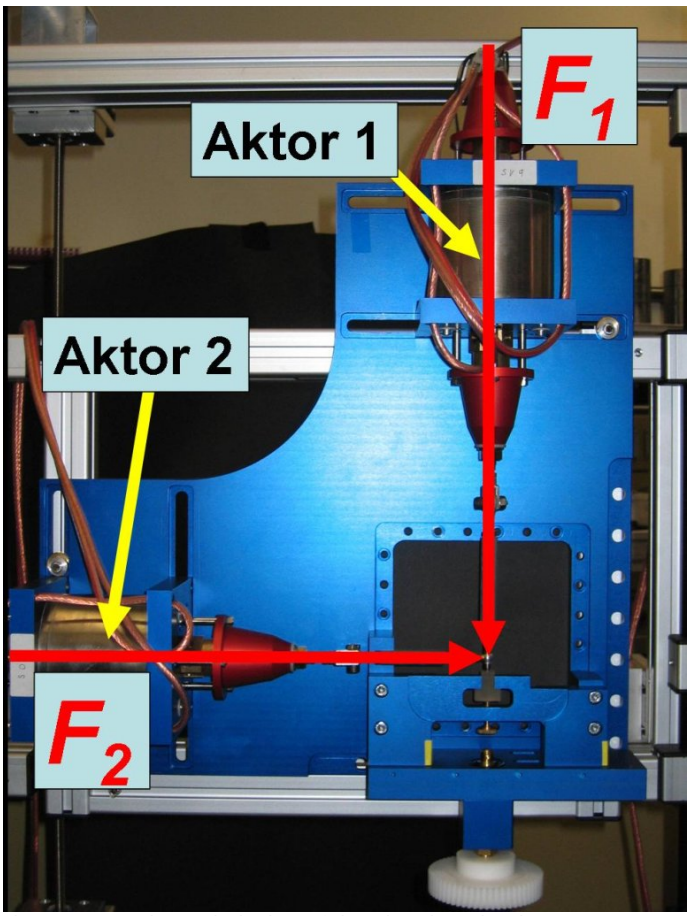

Fig. 31: Overview admission of the chewing simulator.

The force-time-process is variable and adjustable in the used actuators. Both actuators use the Lorenz strength, for which the following formula is the basis.

$$F_{(t)} = i_{(t)} \times l \times B$$

F (t) = time-dependent Kraft (Lorenz Kraft) [N]
i (t) = temporally changeable river [A]
l = effective leader length [mm] B = magnetic flow density [C]

From the mathematical context; there is a relationship between the actuator stream (coil stream) and the produced force. The actuator stream is therefore directly proportional to the produced force. The simultaneous, however independent force production in both force actuators makes for total produced force of between 0-300 Newton possible. The generated force can be introduced in arbitrary directions of +90° to −90° related to the implant axis. The tolerance of the force actuators amounts to 0.5%. This was determined with force sensors. The two force actuators are controlled through an electronic amplifier (www.willburger.de). The control of the amplifier is driven through a digitally/similar transducer map (company national instrument, type NI USB 6229), which is controlled and directed by the use of the graphic programming system LabVIEW® (www.ni.com). Acceleration changes of the directed force, reaching up to the total force (0.3 N/ms), were achieved by LabVIEW®. Using special force sensors HBM U2B (www.hbm.de); the control system and the produced force are calibrated.

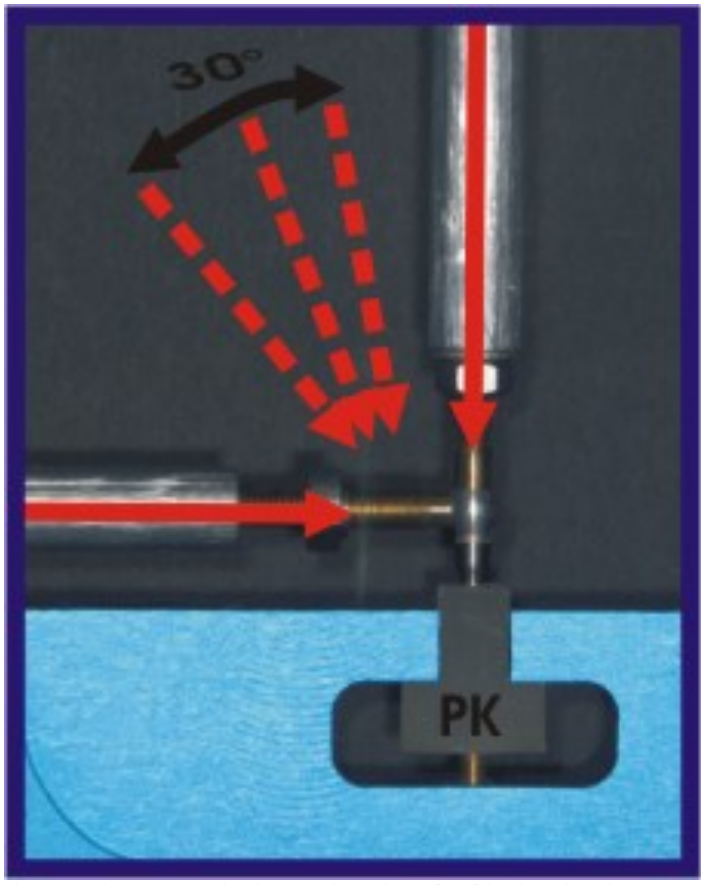

Fig. 32: Close-up of the inspection piece [PK] in the chewing

simulator.

2.6 The radiograph amplifier (RA)

The radiograph amplifier converts the x-ray projection picture into a picture, of wavelength coverage, of visible light. For the herein described study the image amplifier TH 9438 QX from the company Thales (www.thalesgroup.com) was used. The x-ray meets, after entering the radiograph amplifier, an entrance of a fluorescent screen. Scintillation takes place, when the x-ray is converted into visible light. Directly behind the entrance to the fluorescence screen is a photocathode, which sets electrons free through the arriving visible light. The actual amplification effect arises now. The electrons emitted by the photocathode are carried in an electrical field, starting from 60 keV potential differences, and bundled to a higher energy. Now these electrons, which are withdrawn from the radiograph amplifier, meet an output fluorescent screen, which exhibits a clearly smaller surface than the entrance screen. The electrons are made visible through the passage on the output screen. The amplification factor is indicated for this equipment at 200,000 light quanta per x-ray photon. In illustration 33 the schematic structure of the radiograph amplifier TH 9438 QX is represented.

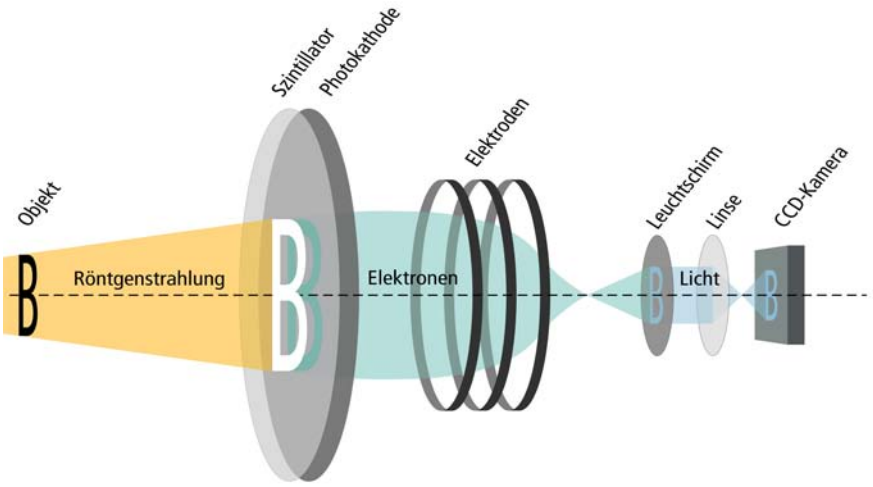

Fig. 33 Schematic structure of the used RA.

2.7 High speed digital camera

The radiograph amplifier follows a High-speed digital camera of the type Redlake Motion Pro® HS-3 (www.redlake.de; Fig. 35).

Fig. 34: High speed digital camera Redlake Motion Pro® HS-3.

This type of camera offers an integrated CCD sensor (load Couplet DEVICE sensor). A CCD sensor sends a digital signal proportional to the irradiated quantity of light. The camera is connected by an USB interface to a computer. The digital camera used here can achieve 1000 pictures per second. The arriving signals were “rushed“. By averaging each individual pixel, of several one behind the other noted pictures, the signal noise could be reduced. The number of pictures, which are charged with one another, is limited by the arising in-motion unsharpness. The highest image quality was reached with the mean calculation of 11 successive pictures. The calculation of the pictures took place via a developed computer program in LabVIEW® (www.ni.com). Fig. 35 represents an exemplarily calculation of 11 pictures, fig. 36 to a and b in each case a non-calculated and a calculated picture.

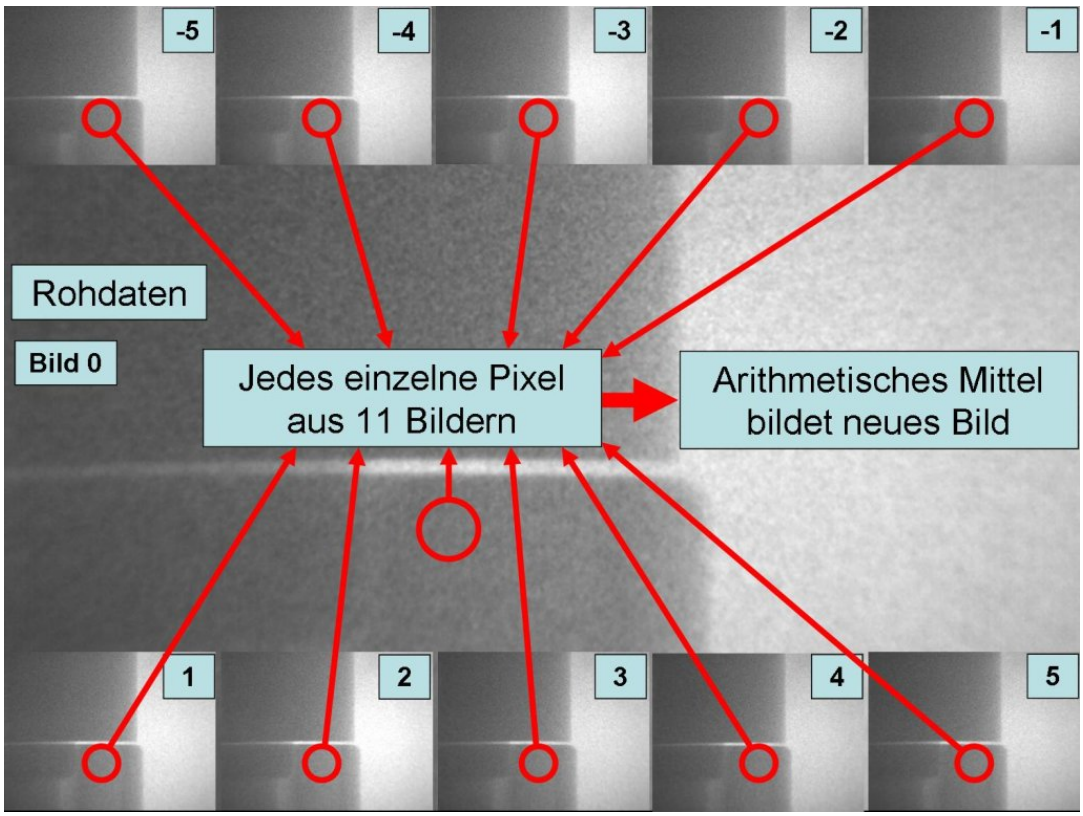

Fig. 35: calculation of picture.

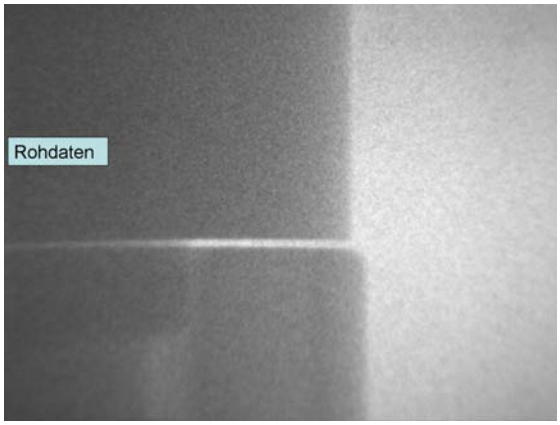

Fig. 36a: Not calculated picture (raw data).

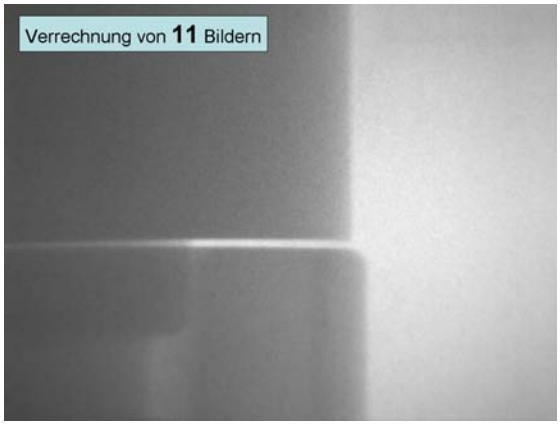

Fig. 36b: Picture after calculation of 11 pictures.

The high image frequency makes for the production of videos, alongside the recording of frames also, possible. The controll of the camera is guaranteed with the help of the graphic programming system LabVIEW® (www.ni.com). The clock frequency, the exposure time and the number of pictures can be adjusted reproducibly. The actuators of the chewing simulator were likewise controlled through and by LabVIEW®, wherein a synchronization of the actuators and the camera took place.

2.8 Load arrangement

All inspection pieces were loaded with forces by 25N, 50N, 75N, 100N, 125N, 150N, 175N, 200N. The axial force vector ($\mathbf{F}_{axial}$) was increased up to the, before defined, force. The inclination of the resulting force vector (**F**resultant) from 30° to the implant axis took place via a force application of the horizontal force vector ($\mathbf{F}_{horizontal}$), represented in fig. 37.

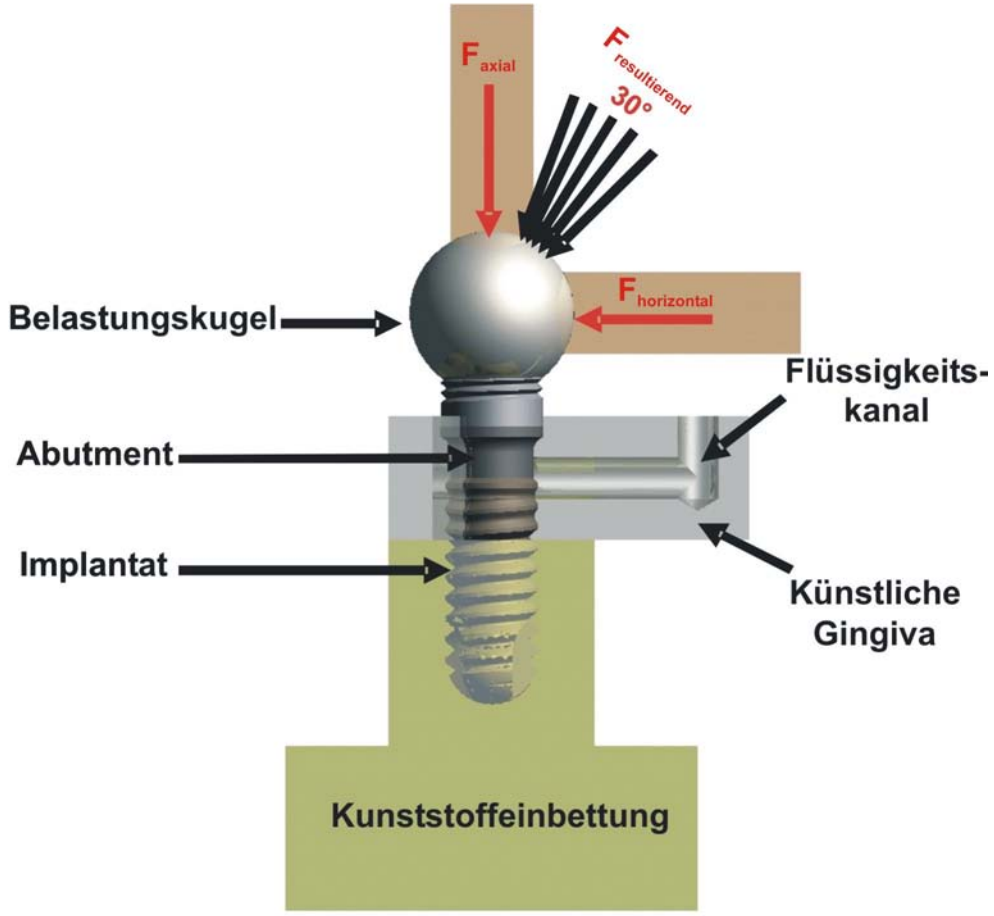

Fig. 37: Schematic representation of the load arrangement.

In the first part of the experiment all inspection pieces were first loaded without an x-ray contrast liquid. In the second part of the investigation; the inside of each individual liquid entrance and artificial mucous membrane was filled with the x-ray contrast liquid. The liquid channel was sealed, after filling, with a sealant rod. Subsequently, all inspection pieces were loaded again under 25N, 50N, 75N, 100N, 125N, 175N, 200N.

2.9 Evaluation

The high image frequency makes it possible to provide x-ray videos. For this; every tenth picture was used. The rate of change in the chewing simulator and the produced force, reaching up to the total force amounts of 0.3 N/ms, whereas the rate of change amounts to 0.6 N/ms, to reach the zero point. The period of time that the axial actuator takes to reach the total force amount was equal to the period during the inclination of the force. From this; results the total time of an inspection piece per force cycle. The load cycle determines the recording time of the camera. Synchronization between the actuators and the camera over LabVIEW® under Microsoft Windows XP is not accurate and therefore it was necessary to include an added and an overhanging time for each cycle period. Preliminary tests resulted in an added time of 100 pictures and an overhang time of 1000 pictures. For example a load of 200N results in a load period of 1.66 seconds. The frequency of 1000 pictures, per second, leads to the admission of altogether 2766 pictures. For the production of the x-ray video as "avi.file" with LabVIEW® (www.ni.com) 276 pictures are used after calculations. The x-ray video corresponds to quadruple the slow motion and makes the evaluation of the dynamic processes at the Implant-Abutment-Interface possible. The existence of a possible micro pump effect could be examined by the behavior of the contrast medium in the x-ray device, which can be distinguished from the remaining structures (implant, abutment, artificial mucous membrane). The evaluation of all provided radiographs and x-ray videos were made visually. The visual evaluation of the frames and the provided x-ray videos, during the load without x-ray contrast medium, were evaluated for an existing micro gap between the implant and abutment. Existing cyclic openings and closings of the micro gap could be made visible. In order to measure the developed gap the frame, during and at its' maximum load, was determined. In this frame each pixel inside the gap was counted. According to the resolution of the x-ray video one pixel corresponds to 1,8µm. Therefore the exact size of an existing gap was specified.

The evaluation of provided pictures and x-ray videos, after load and with brought in x-ray contrast medium, were made likewise visual.

3 Results

The results of the here described study are represented in the following charts. According to the investigational procedure, the occurrence of a micro gap between the implant and the Abutment is shown first. Subsequently, the results of the evaluation and the existance of a micro-pump-effect at Implant-Abutment-Interface are represented.

Tab. 4 shows the results of the microgap. For each inspection piece the picture of maximum load is shown.

Micro-gap Konus K3Pro					
Load	**Inspection piece 1**	**Inspection piece 2**	**Inspection piece 3**	**Inspection piece 4**	**Inspection piece 5**
25N	no space 550	no space 560	no space 555	no space 550	no space 545
50N	no space 760	no space 765	no space 760	no space 770	no space 760
75N	no space 955	no space 955	no space 940	no space 960	no space 950
100N	no space 1050	no space 1060	no space 1055	no space 1060	no space 1060
125N	no space 1190	no space 1185	no space 1195	no space 1185	no space 1180
150N	no space 1385	no space 1380	no space 1390	no space 1380	no space 1380
175N	no space 1590	no space 1580	no space 1595	no space 1590	no space 1590
200N	no space 1745	no space 1745	no space 1780	no space 1760	no space 1765

Tab.4 results of micro gap on picture no.

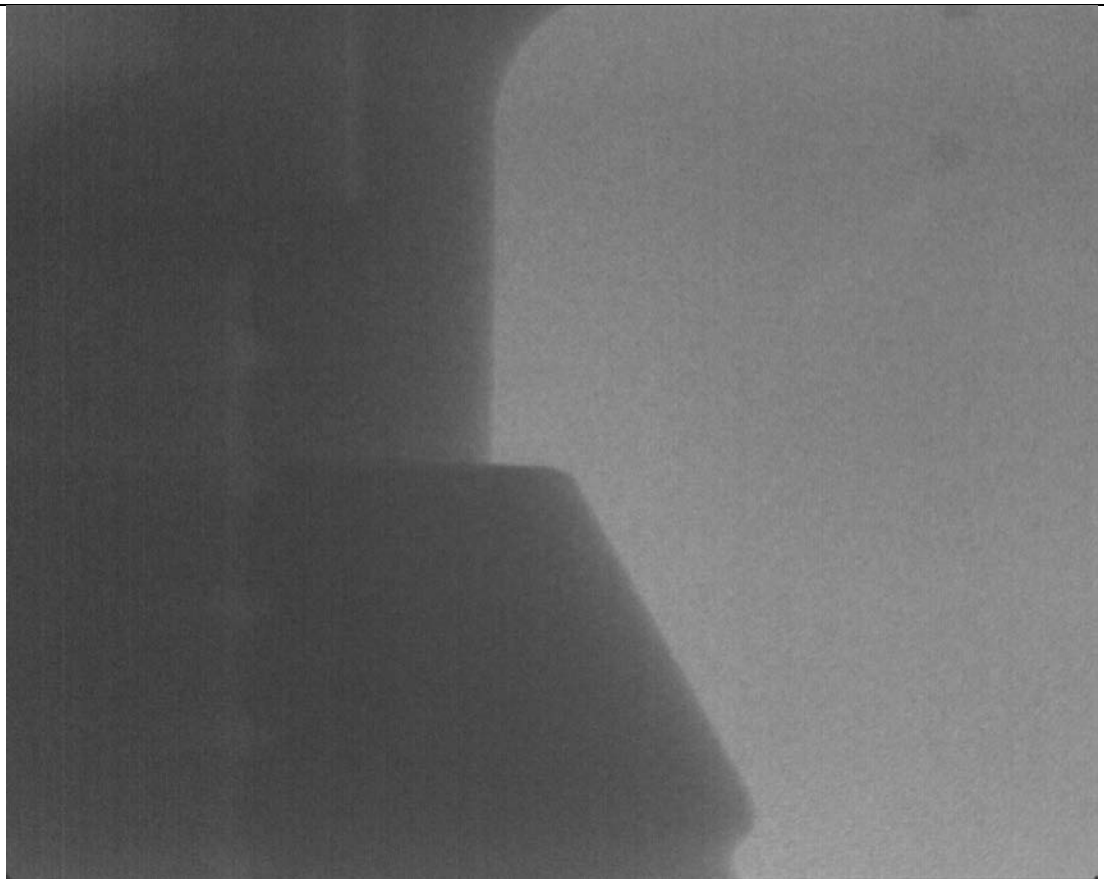

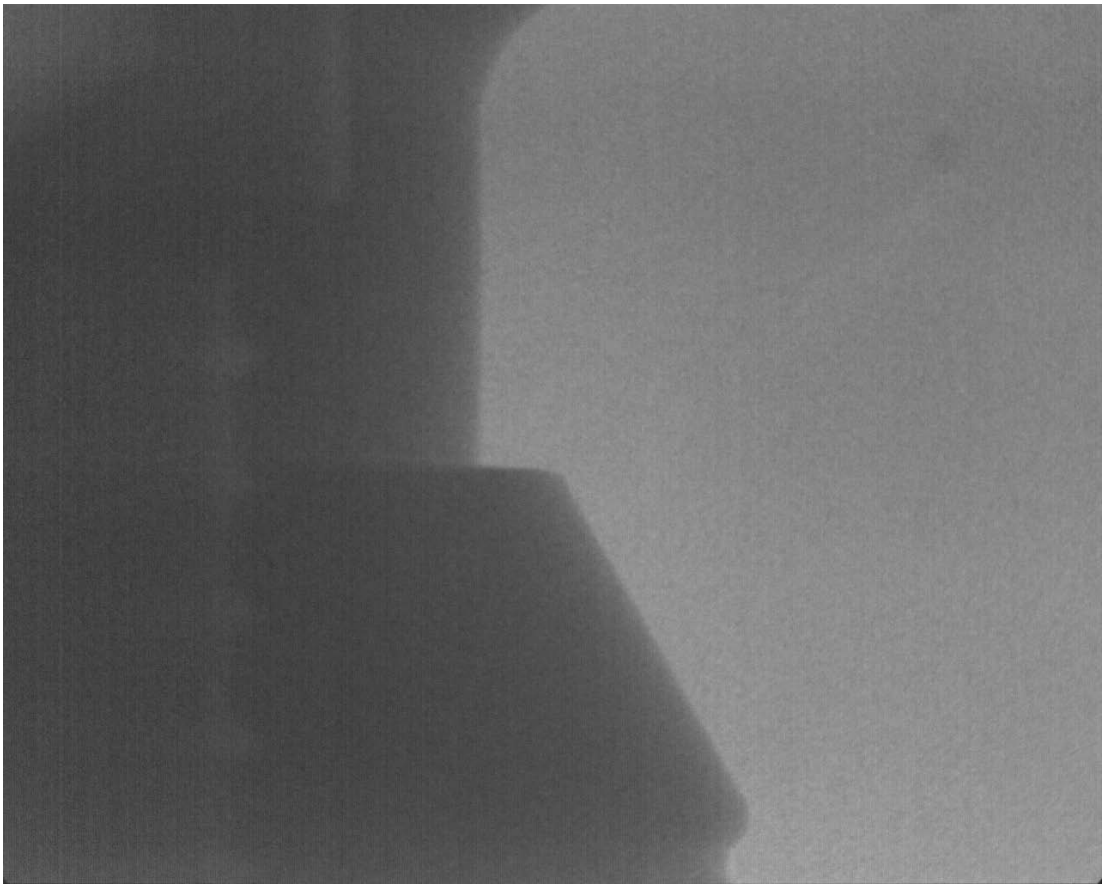

Inspection piece 1; picture no. 1 / 0N; picture no. 1745 / 200N

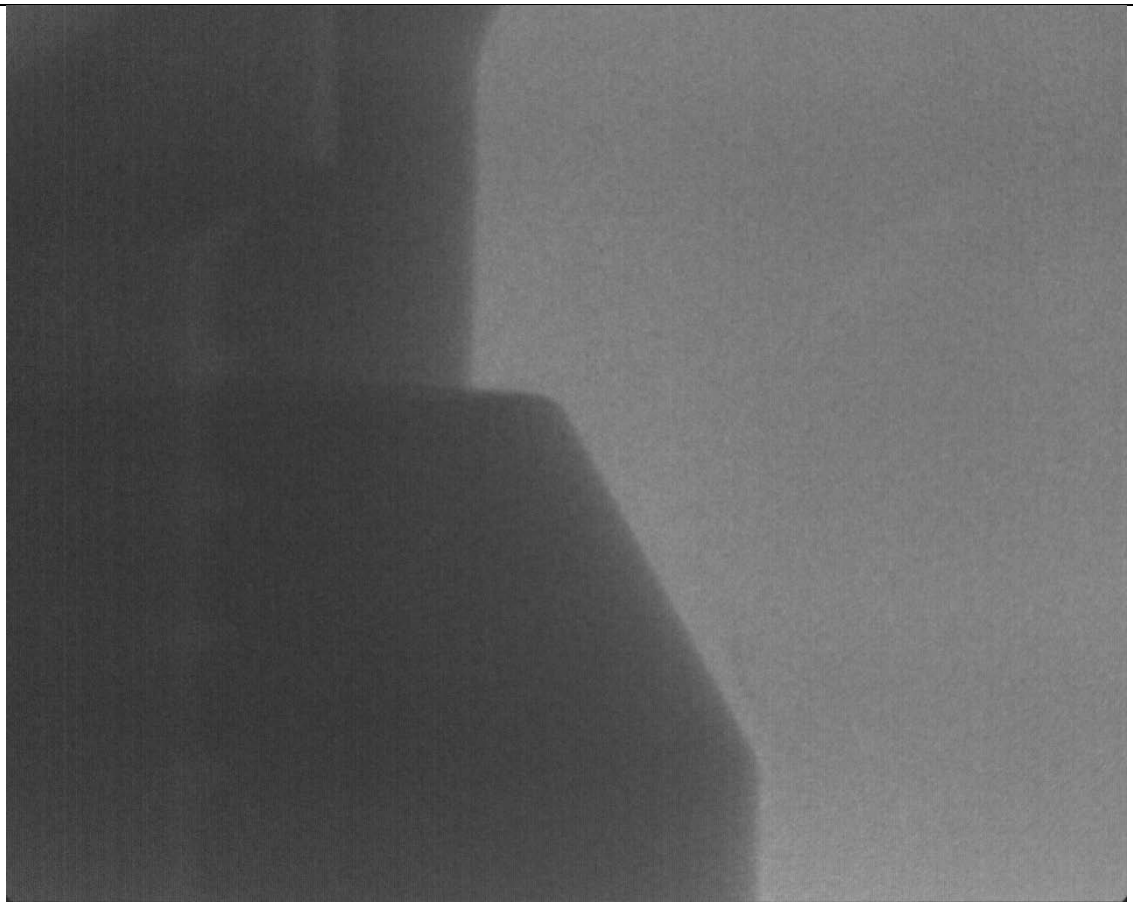

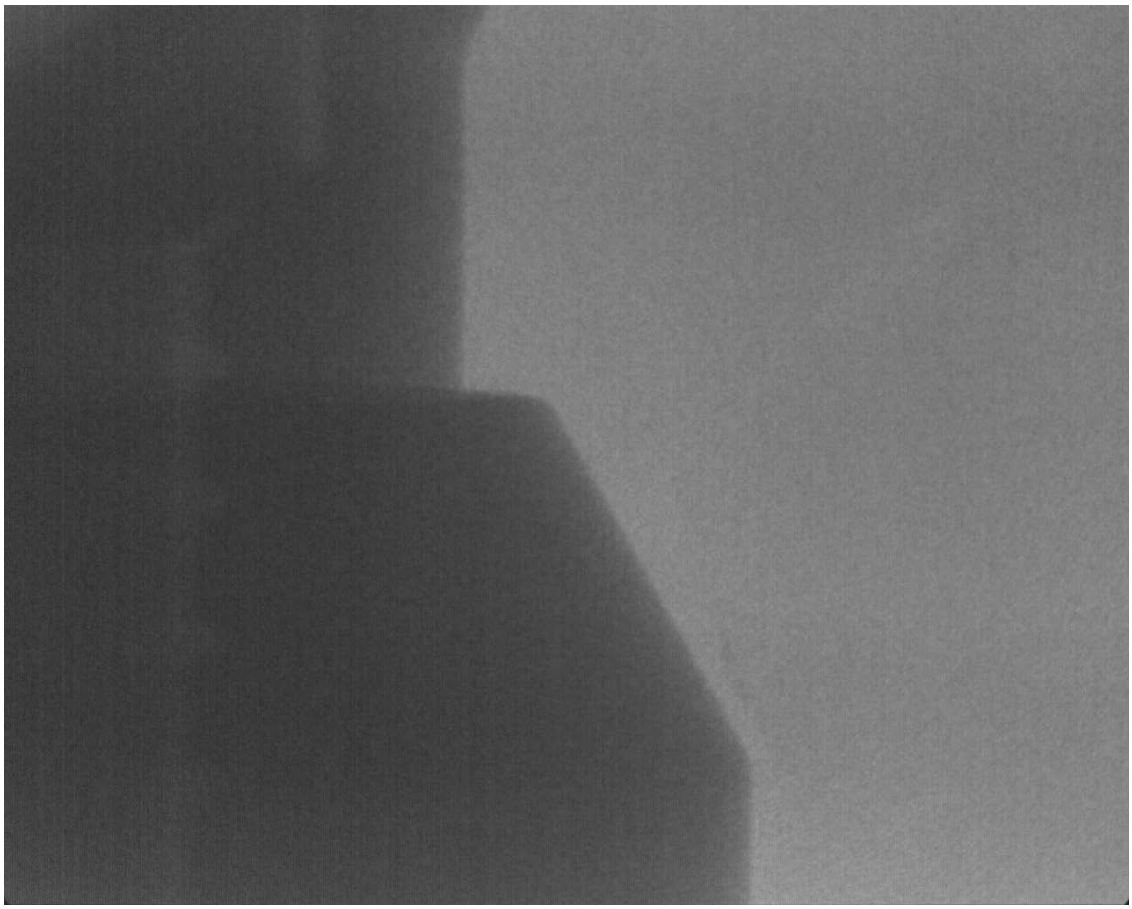

Inspection piece 2; picture no. 1 / 0N; picture no. 1745 / 200N

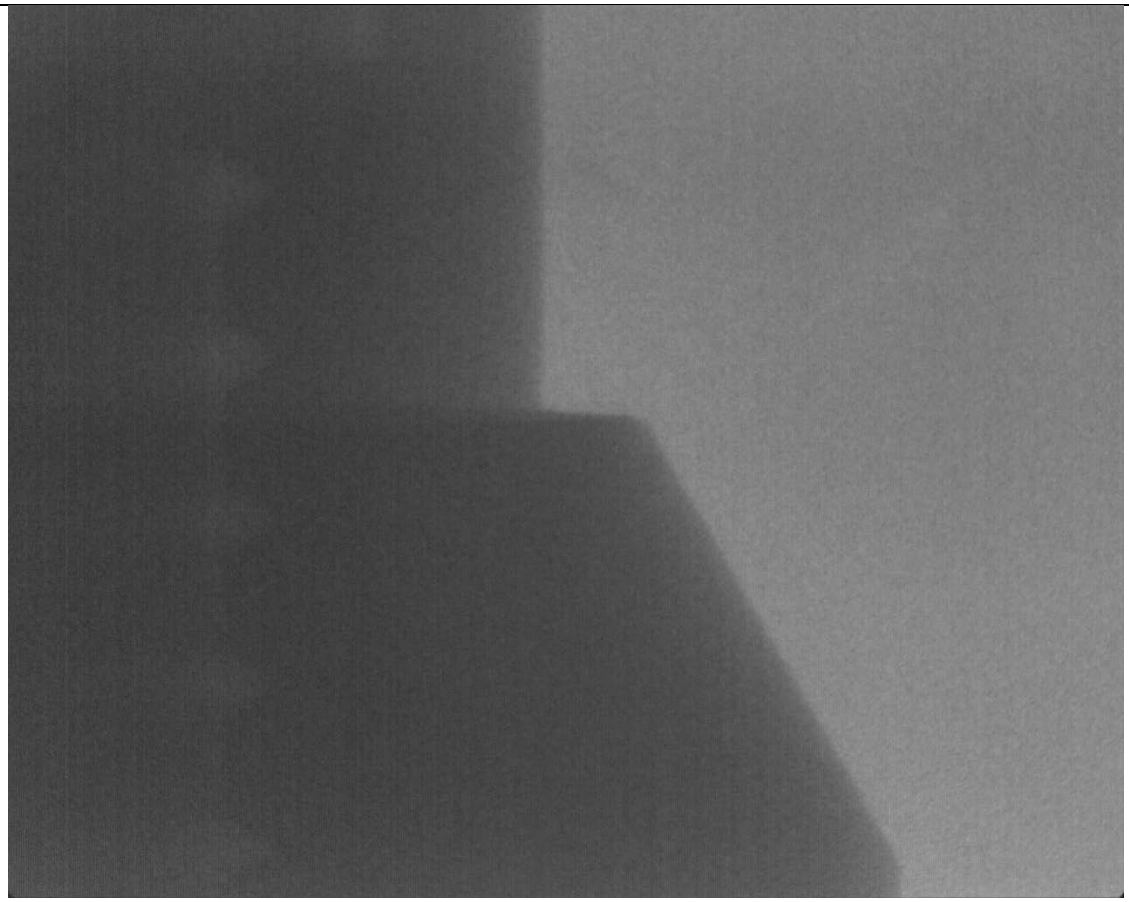

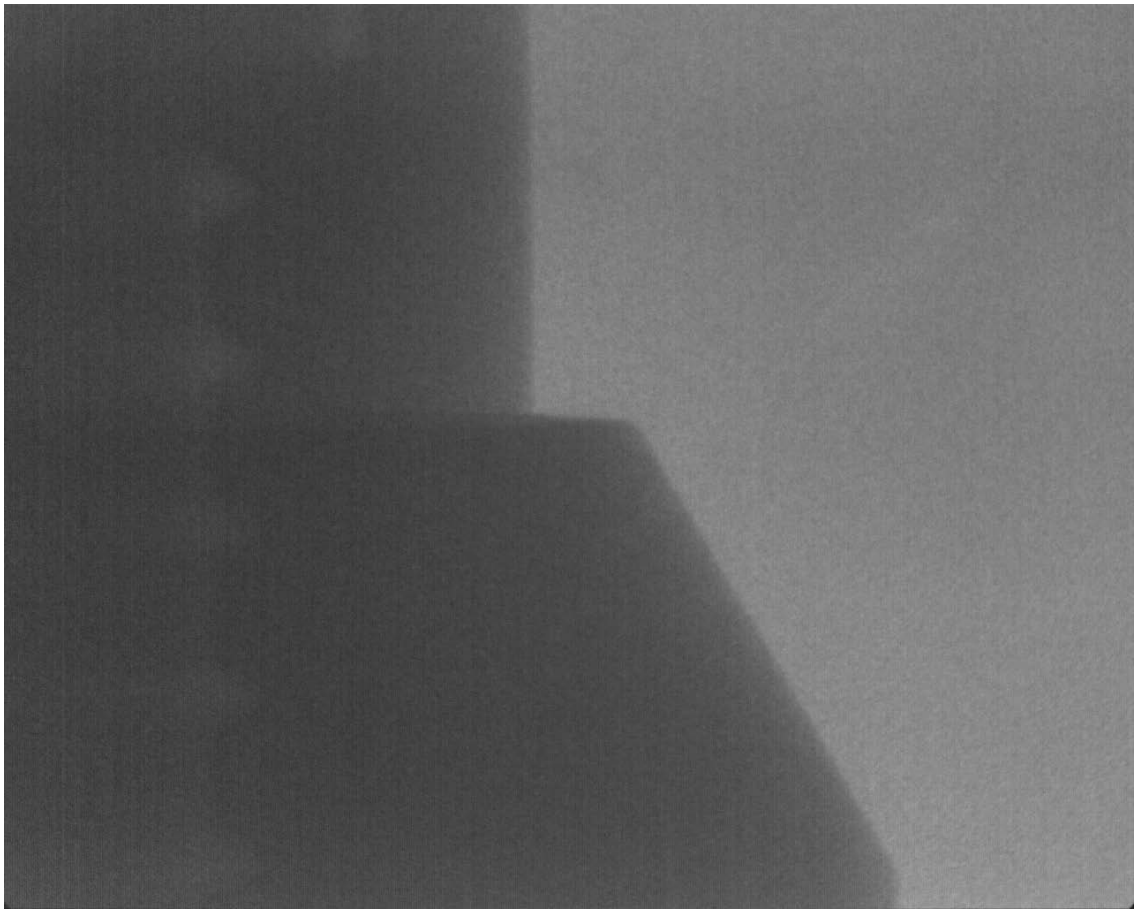

Inspection piece 3; picture no. 1 / 0N; picture no. 1780 / 200N

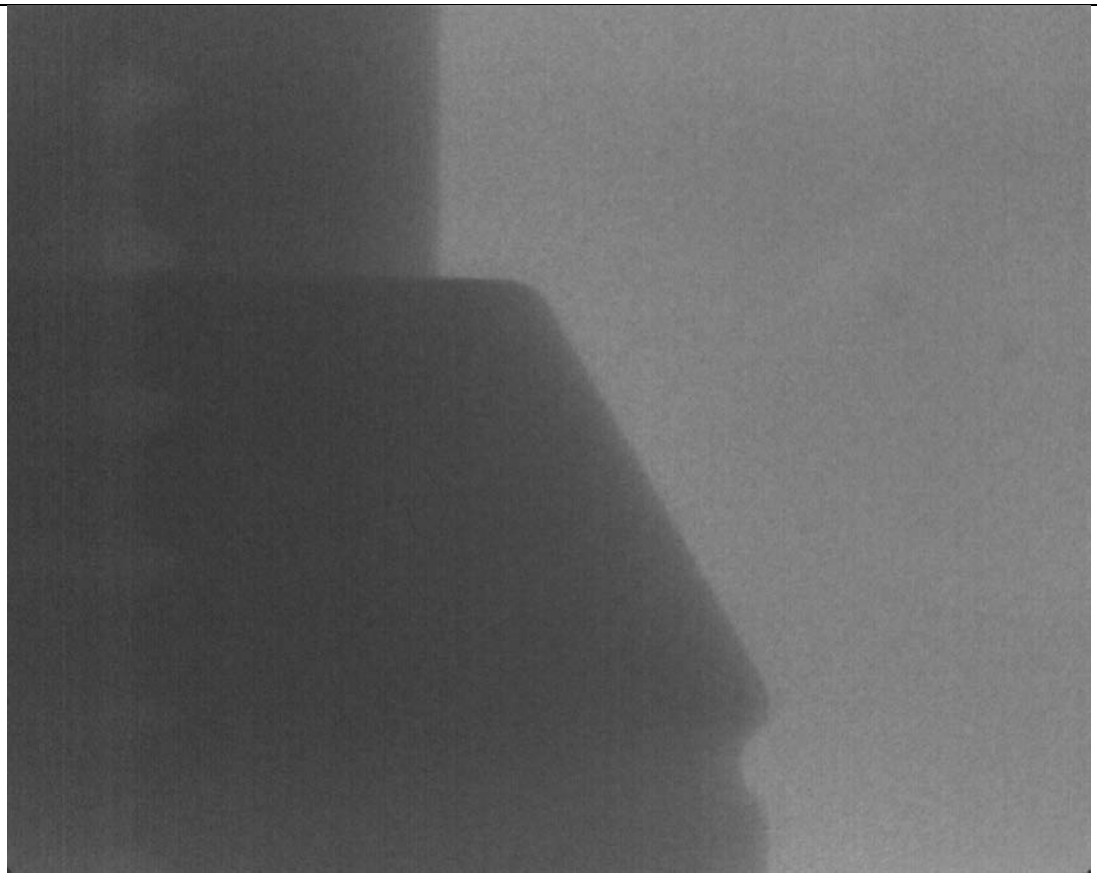

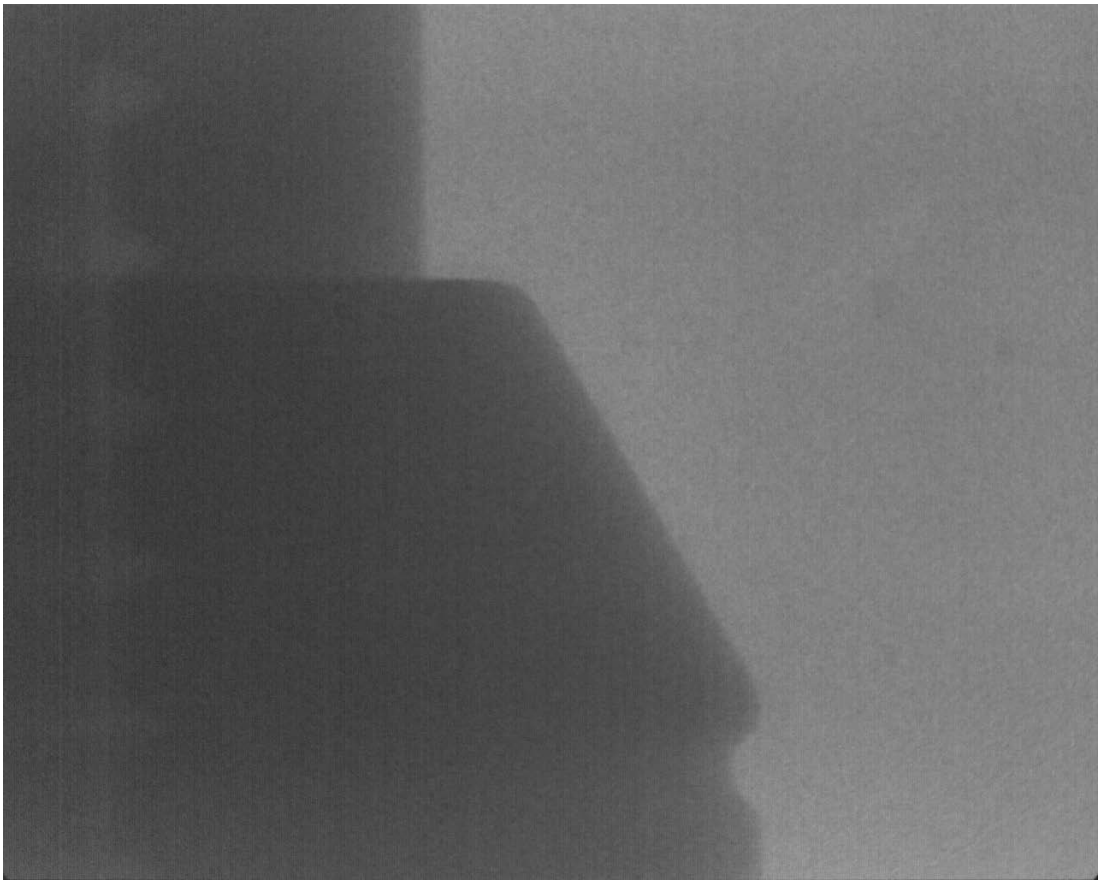

Inspection piece 4; picture no. 1 / 0N; picture no. 1760 / 200N

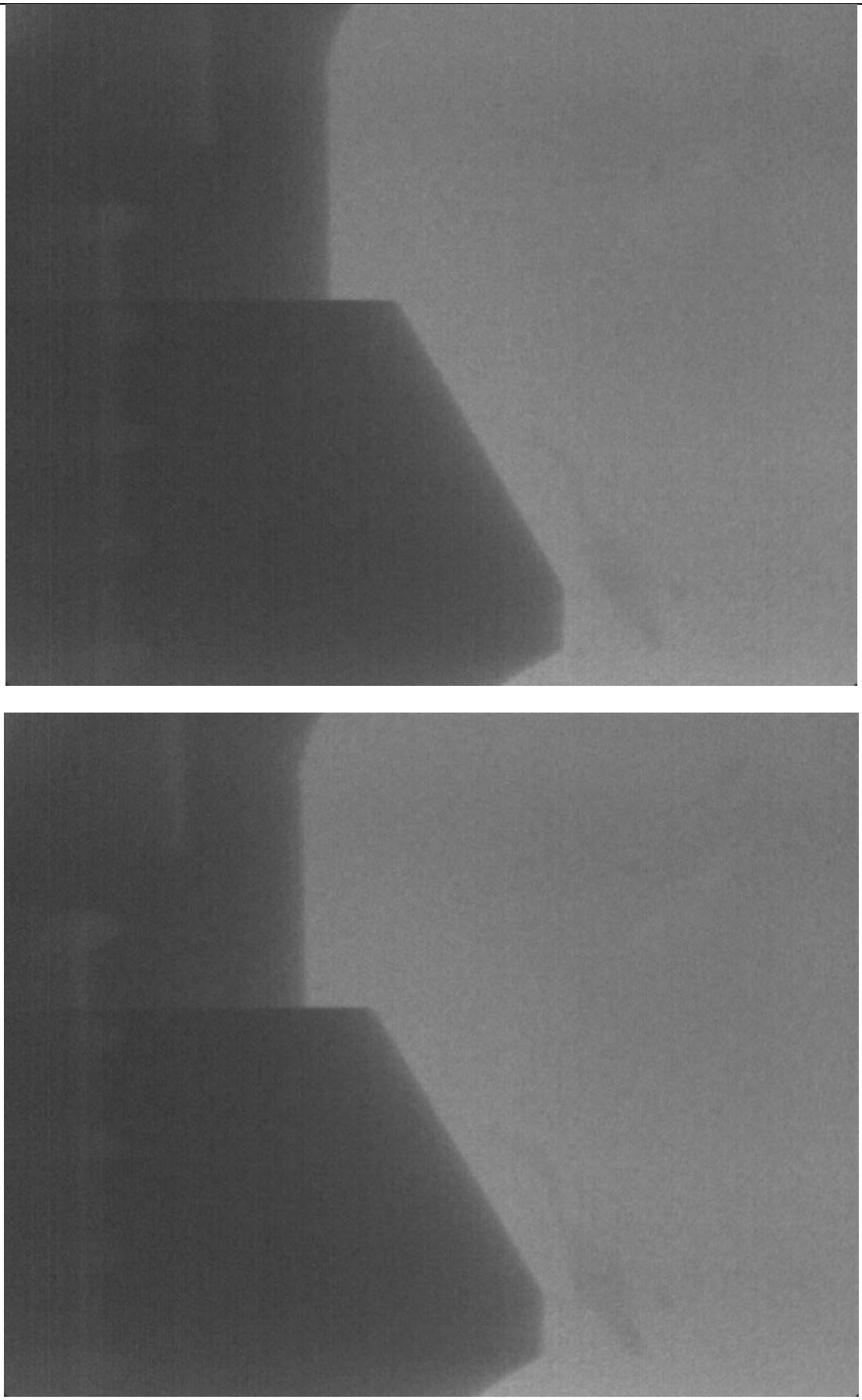

Inspection piece 5; picture no. 1 / 0N; picture no. 1765 / 200N

Micro-pump-effect Konus K3Pro					
Load	**Inspection piece 1**	**Inspection piece 2**	**Inspection piece 3**	**Inspection piece 4**	**Inspection piece 5**
25N	no micro-pump-effect 545	no micro-pump-effect 565	no micro-pump-effect 550	no micro-pump-effect 555	no micro-pump-effect 560
50N	no micro-pump-effect 770	no micro-pump-effect 755	no micro-pump-effect 760	no micro-pump-effect 750	no micro-pump-effect 750
75N	no micro-pump-effect 965	no micro-pump-effect 945	no micro-pump-effect 960	no micro-pump-effect 955	no micro-pump-effect 950
100N	no micro-pump-effect 1060	no micro-pump-effect 1065	no micro-pump-effect 1050	no micro-pump-effect 1045	no micro-pump-effect 1055
125N	no micro-pump-effect 1180	no micro-pump-effect 1195	no micro-pump-effect 1180	no micro-pump-effect 1185	no micro-pump-effect 1190
150N	no micro-pump-effect 1385	no micro-pump-effect 1375	no micro-pump-effect 1385	no micro-pump-effect 1390	no micro-pump-effect 1385
175N	no micro-pump-effect 1580	no micro-pump-effect 1570	no micro-pump-effect 1585	no micro-pump-effect 1575	no micro-pump-effect 1580
200N	no micro-pump-effect 1740	no micro-pump-effect 1760	no micro-pump-effect 1775	no micro-pump-effect 1750	no micro-pump-effect 1760

Tab. 5 results micro pump effect

The results of these in-vitro investigation show that between the tested implant and Abutment no micro space exists. Beyond that no micro pump effect exists.